Predicting flashback limits in H_2 enriched CH_4/Air and C_3H_8/Air laminar flames

Enrique Flores-Montoya[a], Andrea Aniello[a], Thierry Schuller[a], Laurent Selle[a]

[a]*Institut de Mécanique des Fluides de Toulouse, Université de Toulouse, CNRS, Toulouse, France*

Abstract

The influence of hydrogen blending on the flashback limit of dihedral premixed laminar flames stabilized on a slit burner is investigated via two-dimensional direct numerical simulations with conjugate heat transfer and detailed chemistry. Flashback limits are determined for CH_4/H_2/Air and C_3H_8/H_2/Air mixtures with hydrogen contents ranging from 0 % to 100 % and varying fuel-to-air ratios adjusted according to the iso–T_{ad} and the iso–δ_T hybridization strategies. The analysis reveals the existence of two different flashback regimes and a critical effective Lewis number for the fuel mixture, $\mathrm{Le}_c = 0.5$, controlling the switch from one regime to the other. Simulations are also used to explore the dynamics of flames during flashback in these two regimes. They show that for mixtures above the critical effective Lewis number, flashback is symmetric whereas for mixtures below the critical value, an asymmetric flame propagation is observed through the burner slit. These results highlight the impact of preferential diffusion on the stabilization mechanism of hydrogen fuel blends.

Keywords: Fuel Flexible Burners, Preferential Diffusion, Hybridization Strategies, Flashback, Non-equidiffusive Fuels

Novelty and significance statement

1. Definition and application of hybridization strategies to systematically study the effect of hydrogen enrichment and mitigate the downsides of hydrogen admixture in conventional fuels.
2. Observation of two flashback regimes and dynamics in H_2-enriched CH_4/Air and C_3H_8/Air flames.
3. The volume- and diffusion-based effective Lewis number, are found to be controlling parameters in the transition from one flashback regime to the other. A critical value $\mathrm{Le}_c = 0.5$ for the effective Lewis number defines the flashback tipping point and can be used to prevent abnormal flashback.

Author Contribution

E. Flores-Montoya: numerical simulations, analysis, writing: original draft.
A. Aniello: analysis, writing: revision and edition.
T. Schuller: analysis, writing: revision and edition.
L. Selle: supervision, conceptualization, analysis, writing: final version.

1. Introduction

There is a strong push towards the use of hydrogen as a low-carbon fuel [1, 2], which can also act as a storage for excess in renewable electricity production [3] via Power-to-Gas (PtG) strategies [4, 5]. The use of pure hydrogen in combustion devices usually requires the development of new burner designs but it is also possible to blend it with conventional fuels, for example via direct injection in Natural Gas (NG) pipelines [6]. It is generally accepted that hydrogen contents of up to 20% in volume can be accommodated by the existing end-use systems with minor adjustments [7]. A number of experimental studies on the impact of hydrogen blending into NG for end-use applications have evaluated the performance of appliances such as cook-top and oven burners under increasing hydrogen contents [8, 9, 10, 11]. In these studies, flashback is found to be the major limitation for hydrogen blending, which can damage the system and is a major safety issue.

Domestic heating accounts for around 65% of final energy consumption of the residential sector in Europe [12, 13]. Premixed combustion systems such as condensing boilers are widely employed for heating purposes. However, limiting the hydrogen content to $\sim$ 20% in volume corresponds to a 7% reduction of the CO_2 emissions per energy unit, which does not allow for a significant decarbonization. Broadening the capacity to accommodate hydrogen of the current domestic appliances could not only boost the use of hydrogen as an energy carrier but also yield a significant reduction of CO_2 emissions.

The deployment of hydrogen requires laminar Fuel Flexible Burners (FFB) that can operate safely and efficiently over a wide range of hydrogen content in the fuel [14, 15]. FFB pose a series of technical challenges that arise from the significant differences in combustion properties between hydrogen and hydrocarbon fuels. First, hydrogen flames feature larger burning velocities and a broader flammability range [16]. Moreover, the difference between its thermal and mass diffusivity makes lean hydrogen flames prone to thermo-diffusive instabilities [17]. This affects the local burning rate and has a direct impact on flame stabilization. In a recent experimental investigation for two laminar premixed burners used in domestic condensing boilers [18], different flashback and blow-off regimes

are reported depending on the hydrogen content and equivalence ratio. The burner wall temperature is also found to be a critical parameter. Finally, hydrogen blending significantly reduces the auto-ignition time [16, 19]. As a result, auto-ignition induced flashback can occur as reported in [20].

The stabilization of premixed flames is mainly driven by the ratio of the flame speed, S_L, and the inlet bulk velocity, U_B. Outside of a given range, there is either flashback or blow-off. Blending hydrogen into hydrocarbon fuels increases S_L thereby promoting flashback if U_B is not increased. It has been observed that hydrogen reduces the turn-down ratio (i.e. the ratio between the maximal and the minimal operating power) of most burners, which is a challenge for the development of FFB. Consequently, there is a need for fundamental understanding of flame stabilization mechanisms in premixed laminar burners operating with fuel blends.

The seminal work of Lewis and Von Elbe [21] provides the first flashback theory for premixed laminar conical flames. When the diameter of the tube, D, is large compared to the flame thermal thickness δ_T, the bulk velocity at flashback U_B^F is proportional to $DS_L/6\delta_T$. The work of Putnam and Jensen [22] further extends the critical velocity gradient theory by accounting for the velocity profile and a parabolic flame speed distribution near the wall. The results are expressed in terms of Peclet numbers for the jet (Pe_j) and flame (Pe_f). Relations between these two dimensionless numbers at flashback are provided for two scenarios: fully ($\mathrm{Pe}_f > 2$) and non-fully ($\mathrm{Pe}_f < 2$) developed flame speed on the tube axis. The theoretical relations are found to successfully collapse a large number of experimental data for ethylene-air, acetylene-oxygen and NG-air mixtures.

The stabilization of laminar premixed flames anchored to flame holders and bluff bodies has been addressed in a number of recent experimental and numerical studies. In [23], the influence of the flame-holder radius on the anchoring mechanisms at blow-off and flashback is analyzed. Several stabilization regimes where reported and the presence of a recirculation zone for large flame-holder radius was found to broaden the blow-off limit. Vance et al. [24] identified heat losses, stretch and preferential diffusion effects as the main mechanisms for flame stabilization behind bluff bodies for H_2-enriched methane-air flames. The contribution of each mechanism to the anchoring of the flame is evaluated via flame stretch theory, and the resulting model predicts the flame displacement velocity. Both [23] and [24] compare the numerical results to experiments and report good agreement.

In a numerical parametric study, Vance et al. [25] proposed an improved model for flashback prediction in hydrogen-air flames. It is first shown that the local stretch rate, K, at the flame base correlates well with the near-wall velocity gradient, g. One can then estimate the local displacement speed as $S_D = S_L + g\mathcal{L}_M$ where $\mathcal{L}_M$ is the Markstein length. Replacing S_L by S_D in the Lewis and Von Elbe model allows the prediction of flashback for a large variety of cases including equivalence ratio variations and different burner geometries. The influence of the wall temperature on the flashback dynamics for hydrogen enriched methane-air flames was analyzed by Kıymaz et al. [26]. Flashback propensity is found to increase with the burner wall temperature and hydrogen content of the mixture. Finally, the work of Vance et al. [27] analyzes the effect of the fuel Lewis number on the stabilization mechanisms of lean-limit laminar flames stabilized on a bluff body. Two different blow-off regimes are therein identified depending on the fuel Lewis number.

With regard to the flashback mechanism, a number of experimental and numerical studies for boundary layer stabilized flames and turbulent swirled burners have reported the presence of reverse flow regions upstream of the flame leading edge [28, 29, 30]. The formation of these reverse flow pockets questions the validity of the boundary layer flashback model from [21], which is based on the hypothesis that the flame does not affect the incoming flow. Overall, these backflow regions are found to increase the flashback velocity. According to Eichler and Sattelmayer [29], in the presence of stable reverse flow pockets, the flashback limits is determined by the thermal quenching of the reaction inside the backflow zone due to strain and heat losses to the wall.

Despite this significant body of work, there is still a lack of practical guidelines to evaluate how the power turn-down ratio of a laminar burner varies as the hydrogen content in the fuel is increased. The objective of this study is therefore to provide a criterion that can predict a priori how the flashback limit of a given laminar burner evolves with hydrogen content depending on the original hydrocarbon admixture nature. First, in Sec. 2, the reference flames and selected strategies for hydrogen addition are presented. Then Sec. 3 describes the numerical methods and configuration and the main results are discussed in Sec. 4.

2. Theoretical background: hybridization strategies

The considered fuel blend F, is a mixture of hydrogen and a generic hydrocarbon fuel:

$$\mathrm{F} = \alpha\mathrm{H_2} + (1-\alpha)\mathrm{C_mH_n}, \tag{1}$$

where α is the molar fraction of hydrogen in F. The global combustion of F with air in lean conditions can be written:

$$\begin{aligned} \alpha\mathrm{H_2} + (1-\alpha)\mathrm{C_mH_n} + \\ \frac{1}{\phi}\left(\psi - \frac{\alpha}{2}(2\psi-1)\right)(\mathrm{O_2} + a\mathrm{N_2}) \longrightarrow \\ m(1-\alpha)\mathrm{CO_2} + \left(\frac{n}{2}(1-\alpha)+\alpha\right)\frac{n}{4}\mathrm{H_2O} + \\ a\frac{1}{\phi}\left(\psi - \frac{\alpha}{2}(2\psi-1)\right)\mathrm{N_2} + (\frac{1}{\phi}-1)\left(\psi - \frac{\alpha}{2}(2\psi-1)\right)\mathrm{O_2}. \end{aligned} \tag{2}$$

where ϕ is the equivalence ratio, $a = 3.76$ the molar ratio of nitrogen to oxygen in air and $\psi = m + n/4$. It is also useful to define the fraction of thermal power provided by hydrogen:

$$\alpha_P = \frac{\alpha W_{\mathrm{H_2}} Q_{\mathrm{H_2}}}{\alpha W_{\mathrm{H_2}} Q_{\mathrm{H_2}} + (1-\alpha) W_{\mathrm{C_mH_n}} Q_{\mathrm{C_mH_n}}}, \tag{3}$$

where W_k and Q_k denote the molar mass and the Lower Heating Value of fuel k, respectively. Incidentally, α_P is also equal

to the reduction in CO_2 mass emissions obtained by replacing the combustion of C_mH_n with the combustion of the hydrogen enriched fuel blend F.

The addition of hydrogen in the fuel changes virtually all the characteristics of the flame (speed, thickness, adiabatic temperature, etc.) as well as the thermal power of the system. When α is varied, one can simultaneously alter the equivalence ratio, ϕ, in order to conserve some of these properties. The power can be set independently via the total mass flow rate but one has to bear in mind that this will affect the bulk flow velocity through the burner, U_B, and therefore the flashback limit.

Most domestic boilers powered with natural gas are designed to operate at a roughly constant equivalence ratio over the whole power range. However, in a context where the hydrogen content in the fuel is imposed by external factors (e.g. drop in the gas network, variable local hydrogen production), FFB may need to modulate the air-to-fuel ratio to optimize combustion over their whole operating range. In this context, a *hybridization strategy* determines how the properties of the fresh mixture are varied when hydrogen is added to the fuel. For a given thermal power there is a single free parameter, which is the relation between the equivalence ratio, ϕ, and the hydrogen content, α_P. The relation $\phi(\alpha_P)$ can be used to keep certain properties of the flame or the system constant as the hydrogen content is increased. Several options are considered:

- The adiabatic temperature T_{ad}. Whether the system be a heating device or an engine, the temperature of the burned gases is a first-order parameter on the performance and robustness of the apparatus. One may wish to conserve this quantity or at least to keep it bounded.
- The flame thermal thickness, here defined as $\delta_T = (T_{ad} - T_u)/\max(\partial T/\partial x)$ [31]. It is a major parameter in all theories on flashback limits so one strategy would be to keep it constant.
- The laminar burning velocity S_L. In conventional flame stabilization theories, its ratio with the bulk velocity drives the flame length as well as flashback and blowout limits [21].

The theory of Lewis and Von Elbe [21] states that the flashback limit expressed in terms of U_B/S_L scales with the ratio D/δ_T. According to this model, for an iso–S_L hybridization strategy, the ratio U_B/S_L at flashback would vary as the inverse of the flame thermal thickness, δ_T. In contrast, at constant δ_T, the ratio U_B/S_L should be constant. Therefore, in the iso–δ_T strategy, deviations in the value of U_B/S_L at flashback shed light on the influence of parameters that are not considered in the classical flashback theory of Lewis and Von Elbe. Consequently, the iso–δ_T and the iso–T_{ad} strategies are considered in this work.

Figure 1 shows the evolution of T_{ad} and δ_T versus ϕ and α_P for a one-dimensional unstretched adiabatic methane-hydrogen-air laminar flame. These maps were generated using the Cantera software and an Analytically Reduced Chemistry (ARC) scheme presented in Sec. 3. Iso-lines are drawn in Fig. 1, corresponding to the two considered *hybridization strategies* labeled iso–T_{ad} and iso–δ_T, respectively. While keeping T_{ad} constant yields modest variations in equivalence ratio, keeping the flame thickness constant requires a strong reduction of ϕ as H_2 is added to the fuel mixture.

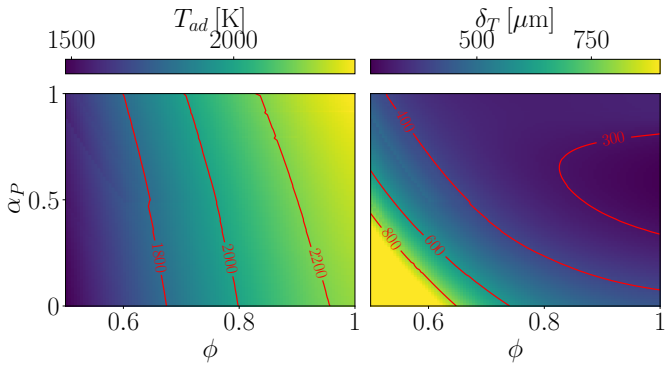

Figure 1: Adiabatic flame temperature T_{ad} and flame thermal thickness δ_T maps for a one-dimensional premixed laminar flame of methane-hydrogen-air as a function of the mixture global equivalence ratio, ϕ, and the hydrogen content expressed as a power fraction, α_P.

A reference operating condition $\phi_0 = \phi(\alpha_P = 0)$ should then be chosen. Typical values for natural gas burners of domestic boilers are in the range $0.7 < \phi_0 < 0.8$ in order to keep NOx emissions low. In this study, the chosen value is $\phi_0 = 0.75$ for propane. For methane, the value of ϕ_0 is set so that the adiabatic flame temperature is the same as that of propane. The reference conditions and the associated flame characteristics are summarized in Tab. 1.

Fuel	ϕ_0	δ_T [μm]	S_L [cm s^{-1}]	T_{ad} [K]
C_3H_8	0.750	482	26.20	1976
CH_4	0.785	546	26.07	1979

Table 1: Properties of one-dimensional unstretched adiabatic C_3H_8 and CH_4 flames at the reference operating point $\alpha_P = 0$.

Once this point has been chosen, one can extract from Fig. 1 the values of ϕ, T_{ad}, S_L and δ_T versus α_P for the two *hybridization strategies* investigated. Figure 2 presents the variation of these quantities with the hydrogen content, α_P, for C_3H_8 and CH_4. Regarding the evolution of ϕ and as anticipated from Fig. 1, while the iso–T_{ad} strategy does not yield a reduction below $\phi = 0.7$, the iso–δ_T requires the equivalence ratio to be reduced as low as 0.45 for pure H_2. Consequently, the adiabatic flame temperature plunges by almost 500 K for the iso–δ_T strategy. This strong variation will affect the burner temperature and consequently the flashback limits. Conversely, while the flame speed is mildly increased in the iso–δ_T strategy, it is multiplied by a factor 5 for the iso–T_{ad} case between $\alpha_P = 0$ and $\alpha_P = 1$. This will surely directly alter the flashback limits. Finally, the flame thermal thickness is reduced by a factor two in the iso–T_{ad} case.

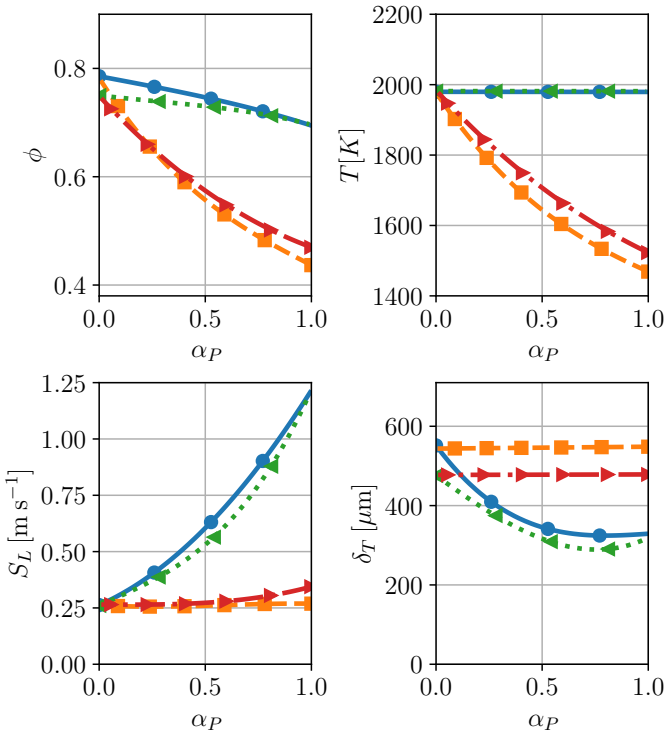

Figure 2: Evolution of equivalence ratio ϕ, laminar burning velocity S_L, thermal thickness δ_T and adiabatic flame temperature T_{ad} versus hydrogen content α_P for the two fuel blends under investigation CH_4/H_2 and C_3H_8/H_2 and the iso–T_{ad} and the iso–δ_T hybridization strategies. —●—: iso–T_{ad} – CH_4; —■—: iso–δ_T – CH_4; —◀—: iso–T_{ad} – C_3H_8; —▶—: iso–δ_T – C_3H_8.

3. Numerical setup

Two-dimensional numerical simulations are now used to determine the flashback limits of methane-hydrogen and propane-hydrogen blends for increasing hydrogen content in a premixed laminar burner. In this Section, the solvers, computational domain and numerical procedure are described.

3.1. Solvers and coupling strategy

The reacting flow is computed using the AVBP software developed by Cerfacs, which solves the compressible Navier-Stokes equations on unstructured meshes. Conjugate heat transfer between the fluid and solid is accounted for via coupling with the AVTP code, which solves the Fourier equation in the solid. This allows accounting for the influence of the burner temperature on the flame stabilization via the preheating of the fresh gases. Radiative heat transfer is not considered in this study. This may not be a strong limitation for domestic burners but in some industrial applications, flames can be very sooty and radiation has a strong contribution to the thermal state of the system. Radiation from the solid remains as an overall loss, which is unaccounted for. This implies that the burner temperature is overestimated in the present simulations, which therefore represent a worse-case scenario in terms of flashback.

Both AVBP and AVTP solvers are unsteady and exchange boundary conditions periodically. AVTP prescribes the solid temperature while AVBP imposes the heat flux from the gaseous phase. This strategy is known as Neumann-Dirichlet coupling and the conditions for its stability are well known [32]. In this work, the objective is to compute steady states until flashback so that the two codes can be de-synchronized in time. This means that between two coupling events, due to the the slow heat transfer controlled by diffusion in the solid phase, the time advancement in the solid is much larger than that in the fluid. This methodology has been extensively validated and successfully applied to the complex case of a gas-turbine blade [33]. More details about the numerics can be found in Appendix A of the Supplementary Material.

3.2. Mesh and boundary conditions

The two-dimensional fluid domain depicted in Fig. 3 allows the stabilization of a laminar flame on a thin slit, which is representative of domestic boiler burners. The geometrical parameters of the burner, namely the slit width $d = 1$ mm, the wall length $w = 1$ mm and the wall thickness $e = 0.5$ mm are kept constant. The total length of the fluid domain is $4h$, with $h = d + w$. Boundary conditions are set using the NSCBC formalism [34]. The velocity $\mathbf{u}_{in}$, temperature, T_{in}, and mixture composition, Y^k_{in}, are set at the inlet and the pressure p_{out} is imposed at the outlet section. No-slip boundary conditions are applied on the inert solid surface. Finally, periodic boundary conditions are applied to the sides. The inlet temperature is set at $T_{in} = 300$ K and the outlet pressure is $p_{out} = 101325$ Pa.

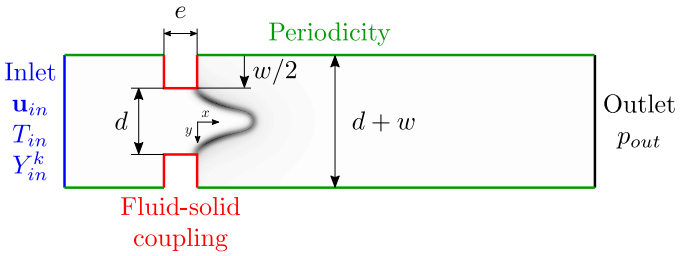

Figure 3: Sketch of the fluid domain, its geometrical parameters, and the applied boundary conditions.

The mesh characteristic size is 20 μm in the fluid and solid domains. This resolution ensures a minimum of 14 points within the flame thermal thickness in the worst case scenario, i.e. the C_3H_8/H_2 fuel blend, $\alpha_P = 80\%$ and iso–T_{ad} strategy. The ARC scheme developed in [35] was used to model the kinetics of methane-hydrogen and propane-hydrogen fuel blends. It involves 22 transported species, 173 reactions and 12 species in quasi-steady state.

3.3. Flashback limit determination

For a given hydrogen fraction α_P, the equivalence ratio ϕ is adjusted according to the fuel blend and the hybridization strategy, which determines the reactants composition Y^k_{in}. For each mixture, a stationary flame at thermal equilibrium with the solid wall is computed. Then, the inlet velocity is reduced in steps corresponding to a decrease of the thermal power by 125 W/m. The flashback limit of a given α_P and ϕ is defined as the smallest

power for which a steady flame can be obtained. This minimal power is designated as flashback limit and denoted by P_f.

4. Results and Discussion

This section is devoted to the analysis of the flames at the flashback limit. Their structure is first examined in order to identify the physical parameters driving the onset of flashback. Then, the dynamics of the flame during flashback is presented.

4.1. Flame front structure

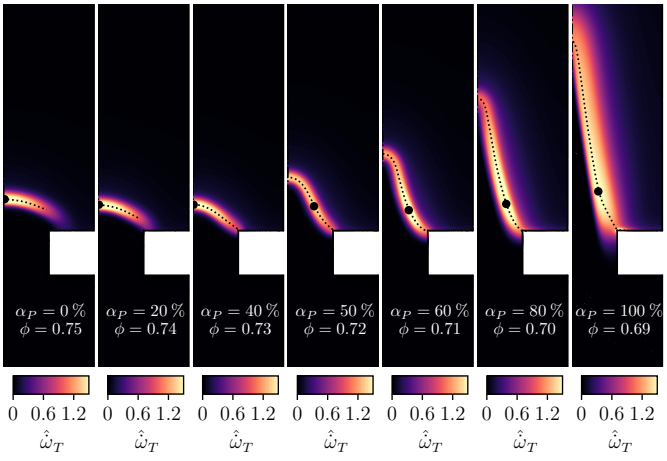

(a) hybridization strategy: iso–T_{ad}

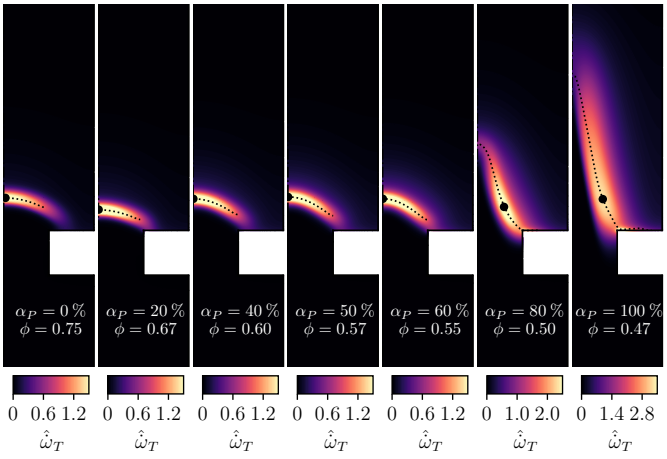

(b) hybridization strategy: iso–δ_T

Figure 4: Normalized heat-release rate for propane-hydrogen-air flames with increasing hydrogen content α_P.

Figure 4 shows the normalized fields of heat release rate at the flashback limit, for H_2-enriched propane-air flames in the iso–T_{ad} and iso–δ_T hybridization strategies. The heat release rate $\dot{\omega}_T$ is normalized by the maximum value in the corresponding one-dimensional unstretched adiabatic flame with the same inlet conditions, $\dot{\omega}_T^0$. All cases are labeled with the hydrogen content α_P and the equivalence ratio, ϕ. The corresponding figure for H_2-enriched methane-air flames can be found in Appendix B of the Supplementary Material. Additionally, the flame front is highlighted via a dotted line, defined as the coordinates (x_f, y_f) where:

$$(\mathbf{u} \cdot \nabla \dot{\omega}_T)_{x_f, y_f} = 0 \tag{4}$$

In this expression, $\mathbf{u}$ and $\dot{\omega}_T$ denote the local velocity and heat release rate respectively. In order to avoid a mathematical indetermination near the walls where the velocity is null, the dotted line is stopped at 85% of $\dot{\omega}_T^0$. This criterion is somewhat arbitrary but does not alter the following qualitative interpretation. Finally, on each flame, the location of the maximum heat release rate is marked with a large filled circle.

In the iso–T_{ad} strategy (Fig. 4(a)), the flame height at the flashback limit is roughly constant until $\alpha_P \sim 40\%$ but then increases rapidly. There is a five-fold increase in flame height between pure propane and pure hydrogen, which means that flashback occurs at higher values of U_B/S_L. Now scrutinizing the location of maximum heat release rate indicated by the large filled circle, it is centered on the slit for $\alpha_P < 40\%$ and is displaced to the side with higher hydrogen enrichment. Interestingly, its height above the slit does not change much when α_P is increased, which is a somewhat unexpected feature. Regarding the iso–δ_T strategy (Fig. 4(b)), the flame height at flashback first decreases between $\alpha_P = 0$ and 20%, followed by a marginal increase until $\alpha_P = 60\%$ and a steep increase. Variations in the distance to the wall of the heat release maxima are slightly more pronounced with respect to the the iso–T_{ad} strategy but this is primarily due to the initial decrease in the flame height for small hydrogen enrichment.

The anchoring of the flame at the edge of the slit is now discussed. Without hydrogen, the flame root is detached from the wall by approximately one flame thickness but as α_P is increased, it re-attaches to the wall. This qualitative difference can be partly attributed to the local enrichment discussed below. The re-attachment occurs at different values of α_P for the two hybridization strategies: $\alpha_P \geq 40\%$ in the iso–T_{ad} case (Fig. 4(a)) versus $\alpha_P \geq 80\%$ for the iso–δ_T (Fig. 4(b)). This difference can be attributed to the reduction of the flame thickness in the iso–T_{ad} strategy, resulting in a reduction of the side-wall quenching distance. The cases with methane shown in Fig. B.1 of the Supplementary Material display a similar trend.

An analysis of the spatial equivalence ratio distribution is intended to shed light on the variations in flame height and heat release rate distribution. The local equivalence ratio is computed as in [27] via:

$$\Phi = \left(\frac{Z_C + Z_H}{Z_O}\right) \Big/ \left(\frac{Z_C + Z_H}{Z_O}\right)_{st} \tag{5}$$

where Z_k denotes the atomic mass fraction of atom k and subscript '*st*' stands for stoichiometric conditions. Figure 5 shows the distribution of local equivalence ratio, normalized by the inlet equivalence ratio, Φ_{inlet}, which highlights the local deviations driven by thermodiffusive effects. The effect of hydrogen

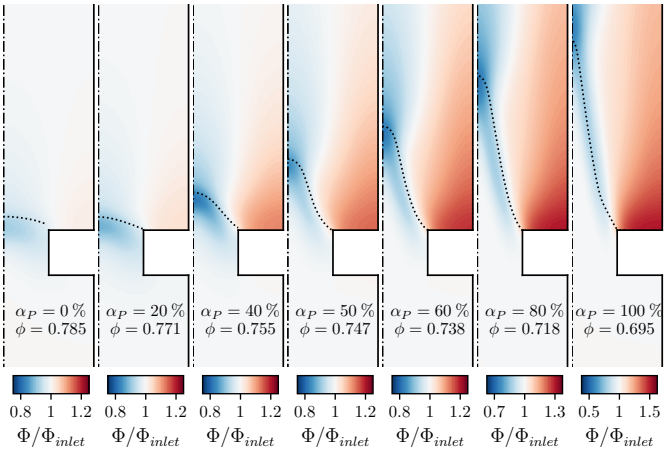

(a) Methane: iso–T_{ad} strategy

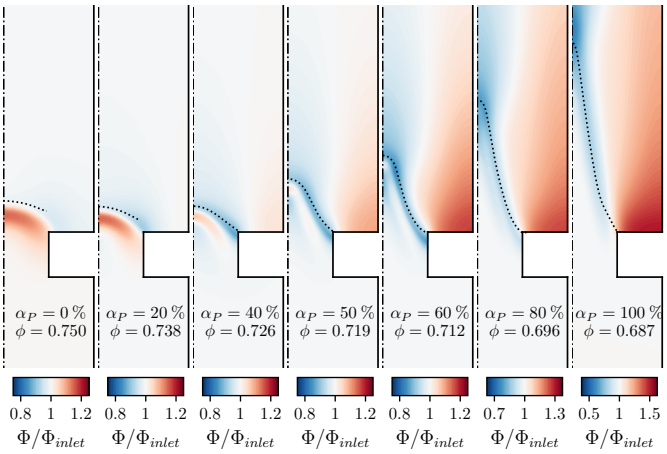

(b) Propane: iso–T_{ad} strategy

Figure 5: Local equivalence ratio, Φ, normalized by its inlet value for flames with increasing hydrogen content, α_P, for the iso–T_{ad} hybridization strategy.

addition on methane and propane flames for the iso–T_{ad} strategy is presented in Fig. 5. The results are qualitatively similar for the iso–δ_T case. For CH_4 (cf. Fig. 5(a)), the fuel Lewis number at $\alpha_P = 0$ is unity so that the normalized local equivalence ratio is roughly constant. As hydrogen is added, Φ reduces on the centerline where the flame is curved towards the fresh gases and increases at the flame base, which has the opposite curvature. This is a typical effect for lean mixtures and is attributed to the small Lewis number of hydrogen Le = 0.316 [36]. For C_3H_8 (cf. Fig. 5(b)) the fuel Lewis number is Le = 1.884, which causes a 20% increase in Φ near the centerline at $\alpha_P = 0$. As the hydrogen content is increased, the effect is compensated by its small Lewis number, with a turning point around $\alpha_P = 50\%$, which corresponds to the increase in flame height. These results suggest that the driving mechanism for the alteration of the flashback limit is the change in fuel Lewis number.

4.2. *Modeling the flashback limit*

Figure 6(a) depicts the evolution of the thermal power at flashback versus α_P for H_2-enriched methane-air and propane-air flames under the two hybridization strategies. This defines the minimal operating power of the burner as a function of α_P. The iso–T_{ad} strategy is discussed first. It is intended to maintain the burnt gas temperature and, therefore, not to affect the thermodynamic cycle of the system as the hydrogen content of the fuel is increased. However Fig. 6(a) shows that with this strategy, the flashback power increases by an order of magnitude when α_P is varied from zero to one. This prevents the operation at low powers for high hydrogen-content and drastically reduces the burner turn-down ratio, should the iso–T_{ad} strategy be chosen. Moving on to the iso–δ_T strategy, the power at flashback is roughly constant until $\alpha_P = 0.6$ but then increases by up to a factor of 5. In the theoretical framework of Lewis and Von Elbe [21], because the ratio D/δ_T is constant in the iso–δ_T strategy, this would attribute the change in flashback limit to the increase in flame speed.

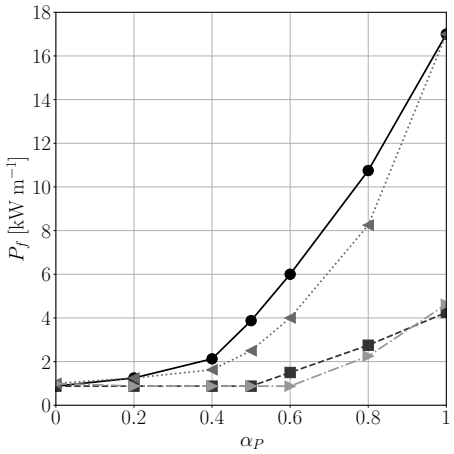

(a) Thermal power at flashback.

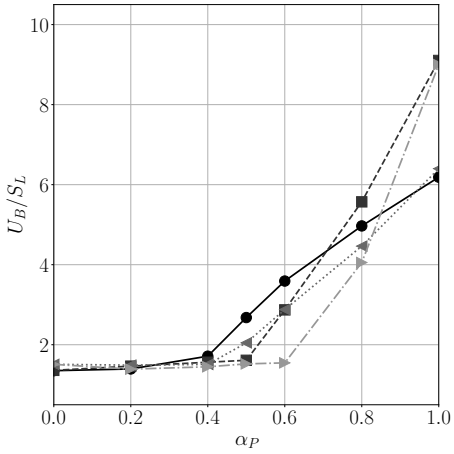

(b) U_B/S_L at flashback.

Figure 6: Evolution of the flashback limit for the different fuel blends and hybridization strategies. —●—: CH_4/H_2 iso–T_{ad}; - -■- -: CH_4/H_2 iso–δ_T; ···◀···: C_3H_8/H_2 iso–T_{ad}; -·▶·-: C_3H_8/H_2 iso–δ_T.

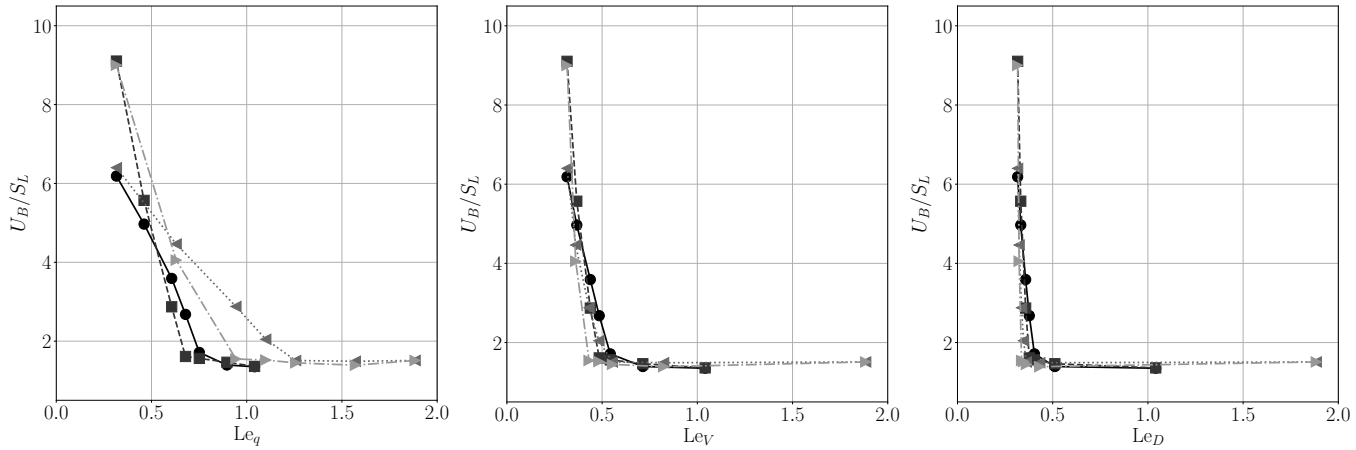

(a) Heat-release-rate averaged Eq. (6) (b) Volume-averaged Eq. (7) (c) Diffusion-based Eq. (8)

Figure 7: Normalized bulk velocity versus effective Lewis number, at the flashback limit for different fuel blends and hybridization strategies. —●—: CH_4/H_2 iso–T_{ad}; -■-: CH_4/H_2 iso–δ_T; ···◀···: C_3H_8/H_2 iso–T_{ad}; -▶·-: C_3H_8/H_2 iso–δ_T.

Overall, Fig. 6(a) shows that the hybridization strategy has a great influence on the flashback limit and that it is similar for both fuels. Because both strategies fail at preserving the flashback limit, one must investigate the evolution of other parameters. In order to remove the influence of the flame speed, the evolution of the normalized bulk velocity U_B/S_L versus α_P is presented in Fig. 6(b).

This ratio remains roughly constant until $\alpha_P = 0.4$ for the iso–T_{ad} strategy and $\alpha_P = 0.6$ for the iso–δ_T strategy. This is similar to the observed evolution of the flame lengths in Fig. 4. This result indicates that the theoretical framework of Lewis and Von Elbe [21] remains valid for low hydrogen content but as anticipated from Fig. 5, past a certain value of α_P, local deviations in equivalence ratio caused by non-unity Lewis number affect the flashback limit.

A criterion for the deviation from the theory of Lewis and Von Elbe, which would not depend on the hybridization strategy is now sought. In the case of multi-fuel blends, various effective-Lewis-number formulations have been proposed to evaluate thermo-diffusive effects [37, 38, 39]. A formulation based on the heat-release rate was proposed by Law et al. [37]:

$$\mathrm{Le}_q = 1 + \frac{\sum_{i=1}^{f} q_i(\mathrm{Le}_i - 1)}{\sum_{i=1}^{f} q_i} \tag{6}$$

where $q_i = Q_i Y_u^i / c_p T_u$ is the normalized heat-release rate, Q_i is the fuel lower heating value per mass unit, Y_u^i is the i-fuel mass fraction, c_p is the specific heat capacity and T_u is the temperature of the reactants. This formulation has been used for example in the analyses conducted in [39, 40, 41, 42]. A second formulation, based on a volume-weighted average was proposed by Muppala et al. [38] and reads:

$$\mathrm{Le}_V = \sum_{i=1}^{f} x_i \mathrm{Le}_i \tag{7}$$

where $x_i = X_i / \sum_{i=1}^{f} X_i$ is the i-fuel volume fraction in the fuel blend $i = 1, \ldots, f$. Finally, a diffusion weighted formulation was proposed by Dinkelacker et al. [39]:

$$\mathrm{Le}_D = \frac{D_T}{\sum_{i=1}^{f} x_i D_{i,\mathrm{N_2}}} \tag{8}$$

where $D_{i,\mathrm{N_2}}$ is the molecular diffusion coefficient of fuel species i in N_2. These formulations have been systematically compared in various related works [43, 44, 39]. The volume-weighted average proposed by Muppala et al. [38] was shown to be well suited to describe the evolution of the Markstein length for H_2/CH_4 and H_2/C_3H_8 blends [43]. Dinkelacker et al. [39] found that the diffusion based formulation, Le_D, yielded better predictions of the flame height in premixed turbulent H_2/CH_4/Air flames for different pressure levels. Similarly, Zitouni et al. [44] reported that the diffusion-based formulation was able to better capture stretch effects on spherical expanding flames for hydrogen enriched CH_4/Air mixtures.

The evolution of U_B/S_L at the flashback limit versus these three formulations for the effective Lewis number is represented in Fig. 7.

Regarding the heat-release-rate averaged formulation (cf. Eq. 6), Fig. 7(a) shows that as Le_q decreases, the flashback limit is pushed to higher values of U_B/S_L but all fuels and hybridization strategies have a different behavior. The volume-averaged effective Lewis number deduced from Eq. (7) and shown in Fig. 7(b) provides a good collapse of all the curves. Above $\mathrm{Le}_V \gtrsim 0.5$ the flashback limit in terms of U_B/S_L is unchanged but for $\mathrm{Le}_V < 0.5$, there is a strong increase in the minimum value of U_B/S_L that can be sustained. Finally, the diffusion-based formulation determined with Eq. (8) and presented in Fig. 7(c) achieves an even tighter collapse of all cases, indicating that there might be some generality in the choice of these variables. From a practical perspective, the value of $\mathrm{Le} \simeq 0.5$ for the volume-averaged or diffusion-based effective Lewis number is a tipping point in the flashback behavior of these flames.

It was observed in Fig. 4 that the increase in flame length is concomitant with the deviation of the location of maximum heat release rate away from the symmetry axis of the flame. This phenomenon is further studied in Fig. 8, which plots the dimensionless transverse coordinate of the position of the heat release rate maxima, y/d, versus Le_D. As for the flashback limit, Le_D

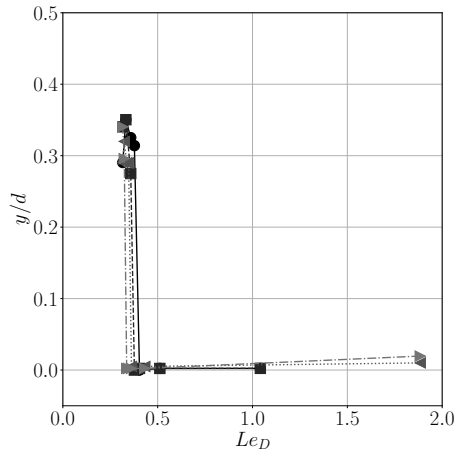

Figure 8: Evolution of the normalized lateral position of the maximum heat release rate versus diffusion-based Lewis number, Le_D, for all cases. —●—: CH_4/H_2 iso–T_{ad}; –■–: CH_4/H_2 iso–δ_T; ···◀···: C_3H_8/H_2 iso–T_{ad}; –·▶·–: C_3H_8/H_2 iso–δ_T.

is a variable that yields a collapse of the curves for all cases: for $\mathrm{Le}_D > 0.5$, the maximum heat release rate is at the flame tip while for $\mathrm{Le}_D < 0.5$ all cases bundle around $y/d = 0.3$. Because the flow velocity decreases for increasing y/d and the local equivalence ratio simultaneously increases (cf. Fig. 5), this explains why flashback occurs at higher values of U_B/S_L for these cases. This effect is quantified by computing the evolution of the displacement speed, S_D, along the flame front:

$$S_D = \frac{\rho}{\rho_u}\mathbf{u}\cdot\mathbf{n}, \tag{9}$$

where $\mathbf{n}$ denotes the unit vector normal to the flame front and ρ is the local density. The displacement speed, S_D, is a measure of the local mass consumption of the flame front [31]. Figure 9 shows the evolution of the displacement speed, S_D, normalized by the laminar burning velocity, S_L, versus the dimensionless transverse coordinate, $2y/d$, for all hydrogen-methane-air flames. For small hydrogen content, the profiles collapse and the maxima is on the symmetry axis. Conversely, for sufficiently high values of α_P, the displacement speed of the flame front develops a local maxima in the vicinity of the flame base. This change in the mass consumption profile along the flame front is responsible for the increase in flashback propensity when the critical Lewis number is reached. Similar observations and conclusions can be drawn for the hydrogen-propane-air flames as shown in Fig. B.2 of the Supplementary Material.

4.3. Flashback dynamics

This section is devoted to the analysis of the flame dynamics during a flashback event. Flashback is the result of an unstable feedback loop between the solid, which heats up when the

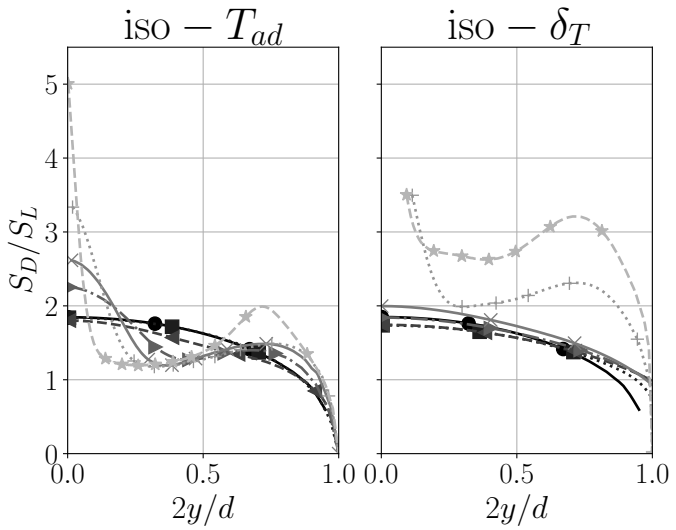

Figure 9: Evolution of the normalized displacement velocity S_D/S_L versus the dimensionless transverse coordinate $2y/d$ for H_2-enriched methane-air flames in the iso–T_{ad} (left) and the iso–δ_T (right) hybridization strategies. —●—: $\alpha_P = 0\%$; ···■···: $\alpha_P = 20\%$; –◀–: $\alpha_P = 40\%$; –·▶·–: $\alpha_P = 50\%$; —×—: $\alpha_P = 60\%$; ···+···: $\alpha_P = 80\%$; –×–: $\alpha_P = 100\%$.

flame gets closer and the flame, which approaches the solid as it heats up. In principle, the numerical simulation of a flashback event would require the synchronization of the combustion and heat transfer solvers [45]. On the one hand, the physical time of this coupling scales with the characteristic time of heat diffusion in the solid, which can be estimated as $t_s = e^2/\alpha \simeq 27.5$ ms, where α is the thermal diffusion coefficient of the solid and e is the thickness of the wall. On the other hand, the flame propagation through the burner slit is a much faster phenomenon with a time-scale of the order of $t_f = e/S_L$, which for the considered cases lies between $0.4 \lesssim t_f \lesssim 2$ ms. Consequently, there is a clear separation of time scales allowing to assume that the solid has a constant – yet nonuniform – temperature during the flashback. Because it is also quite unlikely that the increase in temperature of the burner while the flame is flashing back would drastically affect its dynamics, with the intent to save CPU time, the following procedure is chosen in this work. The initial condition corresponds to the last stable flame that could be obtained with desynchronized coupling, i.e. the flames presented in Sec. 4.1. The temperature of the solid wall is fixed and the inlet velocity is progressively reduced until the flame propagates upstream.

This methodology is now applied to two representative cases: one below and one above the critical threshold of $\mathrm{Le}_V = 0.5$. These flames are respectively $\alpha_P = 20$ % and $\alpha_P = 60$ % for the CH_4/H_2 and the C_3H_8/H_2 blends with the iso–T_{ad} hybridization strategy. Figure 10 shows the flame front dynamics during flashback. In Fig. 10(a), the flame remains symmetric during flashback and the fastest point is the flame tip, corresponding to the location of the maximum heat-release rate when $\mathrm{Le}_V > 0.5$ (cf. Fig. 8). However, as exemplified in Fig. 10(b), when $\mathrm{Le}_V < 0.5$ there is a symmetry breaking and the fastest point in the flame front lies now on the side, which is again

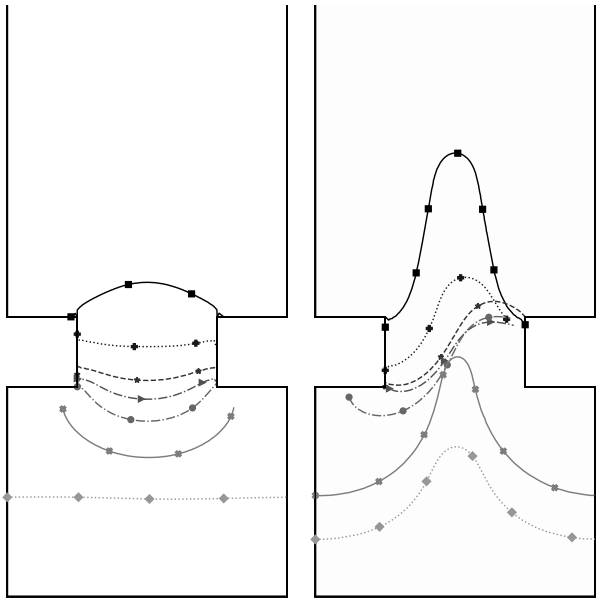

(a) α_P = 20 % (b) α_P = 60 %

Figure 10: Flame front evolution during flashback for the CH_4/H_2 blends with the iso–T_{ad} hybridization strategy. Time step between snapshots is 1.01 ms in a) and 0.45 ms in b).

consistent with the displacement of the location of maximum heat-release rate for high hydrogen content. A similar behavior is observed for the C_3H_8/H_2 flames in Fig. B.3 presented in the Supplementary Material.

Such breaking of symmetry in flame shape has already been reported in numerical simulations [46, 47, 48, 49, 50]. For example in [46, 47], the stabilization of hydrogen-air flames in micro and meso-scale channels with imposed wall temperature profile was shown to be asymmetric for sufficiently large inlet velocities. The transition is found to correspond to the formation of two local maxima of H radical in the flame front. In [48, 49, 50], it is shown that symmetry breaking for flames propagating in narrow tubes allows them to burn more intensively and makes them more robust to quenching.

5. Conclusion

A numerical study on the influence of hydrogen enrichment on methane-air and propane-air flames has been performed. First, the concept of hybridization strategy has been introduced and various hybridization schemes have been considered to set the fresh mixture composition. These strategies define how the fuel-air ratio must be adjusted when the hydrogen content in the fuel is varied in order to preserve the adiabatic flame temperature or the flame thermal thickness. Secondly, two-dimensional direct numerical simulations with conjugate heat transfer have been used to determine the flashback limits of hydrogen-enriched methane-air and propane-air flames in a premixed laminar burner for the two hybridization strategies.

Upon the determination of flashback limits, two different flashback regimes have been identified as the hydrogen content in the combustible admixture is varied. These two flashback regimes are shown to be well correlated with the fuel effective Lewis number based on the volume fraction, Le_V, or the mass diffusion coefficient, Le_D. A critical effective Lewis number of $Le_c = 0.5$ is found to be the tipping point in the flashback limit for all cases. For values above Le_c the flashback velocity of the flame scales with the laminar burning velocity and the maximum of heat release rate is located on the flame symmetry axis. In contrast, for values below Le_c the flame flashback velocity does not scale with the laminar burning velocity and the U_B/S_L ratio increases with the hydrogen content in the fuel. Besides, the flame front features two symmetric local maxima of heat release rate on the flame sides. These results indicate that flashback propensity of hydrogen flames is promoted by preferential diffusion effects and not exclusively linked to their increased flame speed.

Finally, the dynamics of flashback in these two regimes is studied for two representative cases. The simulations reveal two different possible flashback dynamics: a bulk symmetric flashback for low hydrogen contents and an asymmetric flashback for high hydrogen contents.

Acknowledgments

This work was granted access to the HPC resources of IDRIS under the allocation A0132B10627 made by GENCI. The PhD of Enrique Flores Montoya is funded by the company Bulane and the Occitanie Region in the framework of the *Défi Clé Hydrogène Vert*. The financial support of the European Research Council under the European Union's Horizon 2020 research and innovation program Grant Agreement 832248, SCIROCCO is also acknowledged.

References

[1] S. van Renssen, The hydrogen solution?, Nat Clim Chang 10 (2020) 799–801.

[2] A. Midilli, M. Ay, I. Dincer, M. A. Rosen, On hydrogen and hydrogen energy strategies: I: current status and needs, Renew Sustain Energy Rev 9 (2005) 255–271.

[3] H. Blanco, A. Faaij, A review at the role of storage in energy systems with a focus on power to gas and long-term storage, Renew Sustain Energy Rev 81 (2018) 1049–1086.

[4] C. Wulf, J. Linßen, P. Zapp, Review of power-to-gas projects in europe, Energy Procedia 155 (2018) 367–378.

[5] G. Gahleitner, Hydrogen from renewable electricity: An international review of power-to-gas pilot plants for stationary applications, Int J Hydrogen Energy 38 (2013) 2039–2061.

[6] M. Deymi-Dashtebayaz, A. Ebrahimi-Moghadam, S. I. Pishbin, M. Pourramezan, Investigating the effect of hydrogen injection on natural gas thermo-physical properties with various compositions, Energy 167 (2019) 235–245.

[7] J. Leicher, J. Schaffert, H. Cigarida, E. Tali, F. Burmeister, A. Giese, R. Albus, K. Görner, S. Carpentier, P. Milin, et al., The impact of hydrogen admixture into natural gas on residential and commercial gas appliances, Energies 15 (2022) 777.

[8] Y. Zhao, V. McDonell, S. Samuelsen, Experimental assessment of the combustion performance of an oven burner operated on pipeline natural gas mixed with hydrogen, Int J Hydrogen Energy 44 (2019) 26049–26062.

[9] Y. Zhao, V. McDonell, S. Samuelsen, Influence of hydrogen addition to pipeline natural gas on the combustion performance of a cooktop burner, Int J Hydrogen Energy 44 (2019) 12239–12253.

[10] Y. Zhao, V. McDonell, S. Samuelsen, Assessment of the combustion performance of a room furnace operating on pipeline natural gas mixed with simulated biogas or hydrogen, Int J Hydrogen Energy 45 (2020) 11368–11379.
[11] S. Choudhury, V. G. McDonell, S. Samuelsen, Combustion performance of low-nox and conventional storage water heaters operated on hydrogen enriched natural gas, Int J Hydrogen Energy 45 (2020) 2405–2417.
[12] F. Schiro, A. Stoppato, A. Benato, Modelling and analyzing the impact of hydrogen enriched natural gas on domestic gas boilers in a decarbonization perspective, Carbon Resources Conversion 3 (2020) 122–129.
[13] G. L. Basso, B. Nastasi, D. A. Garcia, F. Cumo, How to handle the hydrogen enriched natural gas blends in combustion efficiency measurement procedure of conventional and condensing boilers, Energy 123 (2017) 615–636.
[14] G. Richards, M. McMillian, R. Gemmen, W. A. Rogers, S. Cully, Issues for low-emission, fuel-flexible power systems, Prog Energy Combust Sci 27 (2001) 141–169.
[15] T. Lieuwen, V. McDonell, E. Petersen, D. Santavicca, Fuel flexibility influences on premixed combustor blowout, flashback, autoignition, and stability, J Eng Gas Turbine Power 130 (2008).
[16] A. L. Sánchez, F. A. Williams, Recent advances in understanding of flammability characteristics of hydrogen, Prog Energy Combust Sci 41 (2014) 1–55.
[17] L. Berger, A. Attili, H. Pitsch, Intrinsic instabilities in premixed hydrogen flames: Parametric variation of pressure, equivalence ratio, and temperature. part 1-dispersion relations in the linear regime, Combust Flame 240 (2022) 111935.
[18] A. Aniello, T. Poinsot, L. Selle, T. Schuller, Hydrogen substitution of natural-gas in premixed burners and implications for blow-off and flashback limits, Int J Hydrogen Energy 47 (2022) 33067–33081.
[19] L. Boeck, J. Melguizo-Gavilanes, J. Shepherd, Hot surface ignition dynamics in premixed hydrogen–air near the lean flammability limit, Combust Flame 210 (2019) 467–478.
[20] H. Pers, A. Aniello, F. Morisseau, T. Schuller, Autoignition-induced flashback in hydrogen-enriched laminar premixed burners, Int J Hydrogen Energy 48 (2023) 10235–10249.
[21] B. Lewis, G. Von Elbe, Combustion, flames and explosions of gases, Elsevier, 2012.
[22] A. A. Putnam, R. A. Jensen, Application of dimensionless numbers to flash-back and other combustion phenomena, in: Symposium on Combust Flame, and Explosion Phenomena, volume 3, Elsevier, 1948, pp. 89–98.
[23] F. H. Vance, Y. Shoshin, L. de Goey, J. A. van Oijen, Flame stabilization regimes for premixed flames anchored behind cylindrical flame holders, Proc Combust Inst 38 (2021) 1983–1992.
[24] F. H. Vance, Y. Shoshin, L. de Goey, J. A. van Oijen, Quantifying the impact of heat loss, stretch and preferential diffusion effects to the anchoring of bluff body stabilized premixed flames, Combust Flame 237 (2022) 111729.
[25] F. H. Vance, L. de Goey, J. A. van Oijen, Development of a flashback correlation for burner-stabilized hydrogen-air premixed flames, Combust Flame (2022) 112045.
[26] T. B. Kıymaz, E. Böncü, D. Güleryüz, M. Karaca, B. Yılmaz, C. Allouis, İ. Gökalp, Numerical investigations on flashback dynamics of premixed methane-hydrogen-air laminar flames, Int J Hydrogen Energy 47 (2022) 25022–25033.
[27] F. Vance, Y. Shoshin, J. Van Oijen, L. De Goey, Effect of lewis number on premixed laminar lean-limit flames stabilized on a bluff body, Proc Combust Inst 37 (2019) 1663–1672.
[28] A. Gruber, J. H. Chen, D. Valiev, C. K. Law, Direct numerical simulation of premixed flame boundary layer flashback in turbulent channel flow, J Fluid Mech 709 (2012) 516–542.
[29] C. Eichler, T. Sattelmayer, Premixed flame flashback in wall boundary layers studied by long-distance micro-piv, Exp Fluids 52 (2012) 347–360.
[30] C. Heeger, R. Gordon, M. Tummers, T. Sattelmayer, A. Dreizler, Experimental analysis of flashback in lean premixed swirling flames: upstream flame propagation, Exp Fluids 49 (2010) 853–863.
[31] T. Poinsot, D. Veynante, Theoretical and numerical combustion, RT Edwards, Inc., 2005.
[32] M. B. Giles, Stability analysis of numerical interface conditions in fluid–structure thermal analysis, Int J Numer Methods Fluids 25 (1997) 421–436.
[33] F. Duchaine, N. Maheu, V. Moureau, G. Balarac, S. Moreau, Large-eddy simulation and conjugate heat transfer around a low-mach turbine blade, J Turbomach 136 (2014) 051015.
[34] T. J. Poinsot, S. Lelef, Boundary conditions for direct simulations of compressible viscous flows, J Comput Phys 101 (1992) 104–129.
[35] B. Rochette, F. Collin-Bastiani, L. Gicquel, O. Vermorel, D. Veynante, T. Poinsot, Influence of chemical schemes, numerical method and dynamic turbulent combustion modeling on les of premixed turbulent flames, Combust Flame 191 (2018) 417–430.
[36] M. Mizomoto, Y. Asaka, S. Ikai, C. Law, Effects of preferential diffusion on the burning intensity of curved flames, Symp. (Int.) Combust. 20 (1985) 1933–1939.
[37] C. K. Law, G. Jomaas, J. K. Bechtold, Cellular instabilities of expanding hydrogen/propane spherical flames at elevated pressures: theory and experiment, Proc Combust Inst 30 (2005) 159–167.
[38] S. Muppala, M. Nakahara, N. Aluri, H. Kido, J. Wen, M. Papalexandris, Experimental and analytical investigation of the turbulent burning velocity of two-component fuel mixtures of hydrogen, methane and propane, Int J Hydrogen Energy 34 (2009) 9258–9265.
[39] F. Dinkelacker, B. Manickam, S. Muppala, Modelling and simulation of lean premixed turbulent methane/hydrogen/air flames with an effective lewis number approach, Combust Flame 158 (2011) 1742–1749.
[40] E. Hu, Z. Huang, J. He, H. Miao, Experimental and numerical study on laminar burning velocities and flame instabilities of hydrogen–air mixtures at elevated pressures and temperatures, Int J Hydrogen Energy 34 (2009) 8741–8755.
[41] C. Tang, Z. Huang, C. Jin, J. He, J. Wang, X. Wang, H. Miao, Laminar burning velocities and combustion characteristics of propane–hydrogen–air premixed flames, Int J Hydrogen Energy 33 (2008) 4906–4914.
[42] C. Tang, Z. Huang, J. Wang, J. Zheng, Effects of hydrogen addition on cellular instabilities of the spherically expanding propane flames, Int J Hydrogen Energy 34 (2009) 2483–2487.
[43] N. Bouvet, F. Halter, C. Chauveau, Y. Yoon, On the effective lewis number formulations for lean hydrogen/hydrocarbon/air mixtures, Int J Hydrogen Energy 38 (2013) 5949–5960.
[44] S. Zitouni, D. Pugh, A. Crayford, P. Bowen, J. Runyon, Lewis number effects on lean premixed combustion characteristics of multi-component fuel blends, Combust Flame 238 (2022) 111932.
[45] C. Koren, R. Vicquelin, O. Gicquel, Self-adaptive coupling frequency for unsteady coupled conjugate heat transfer simulations, Int J Therm Sci 118 (2017) 340–354.
[46] G. Pizza, C. E. Frouzakis, J. Mantzaras, A. G. Tomboulides, K. Boulouchos, Dynamics of premixed hydrogen/air flames in microchannels, Combust Flame 152 (2008) 433–450.
[47] G. Pizza, C. E. Frouzakis, J. Mantzaras, A. G. Tomboulides, K. Boulouchos, Dynamics of premixed hydrogen/air flames in mesoscale channels, Combust Flame 155 (2008) 2–20.
[48] C. Jiménez, D. Fernández-Galisteo, V. N. Kurdyumov, Flame-acoustics interaction for symmetric and non-symmetric flames propagating in a narrow duct from an open to a closed end, Combust Flame 225 (2021) 499–512.
[49] A. Dejoan, C. Jiménez, V. N. Kurdyumov, Critical conditions for non-symmetric flame propagation in narrow channels: Influence of the flow rate, the thermal expansion, the lewis number and heat-losses, Combust Flame 209 (2019) 430–440.
[50] A. Dejoan, C. Jiménez, D. Martínez-Ruiz, V. Muntean, M. Sánchez-Sanz, V. N. Kurdyumov, Flame propagation in narrow horizontal channels: Impact of the gravity field on the flame shape, Proc Combust Inst 39 (2023) 1535–1543.